

## Simulation and optimization of live fish locomotion in a biomimetic robot fish

<sup>1</sup> M. Abbaspour; <sup>1\*</sup> M. Asadian Ghahferokhi

<sup>1</sup> Department of Mechanical Engineering, Sharif University of Technology (SUT), Tehran, Iran

Received 24 April 2013; revised 20 May 2013; accepted 27 May 2013

**ABSTRACT:** This paper presents simplified hydrodynamics model for a biomimetic robot fish based on quantitative morphological and kinematic parameters of carangiform fish. The motion of four *Pangasius sanitwongsei* with different length and swimming speed were recorded by the digital particle image velocimetry (DPIV) and image processing methods and optimal coefficients of the motion equations and appropriate location of joints are empirically derived. The swimming speed of fish can be adjusted by changing oscillating frequency, amplitude and the length of oscillatory part, respectively. Experimental results show that the oscillating amplitude increases dramatically from 1/3 of body and is very small near the head. So the second order function which describes wave amplitude of *Pangasius sanitwongsei* undulatory movement equation was found and the oscillatory motion of the biomimetic robot fish will be simulated according to this equation.

**Keywords:** Biomimetic robot fish; Carangiform fish; hydrodynamics; caudal fin; DPIV

### INTRODUCTION

In nature, the belief that plants and animals evolved optimal solutions for survival can be applied to solve engineering problems. For many years robotics researchers have been impressed by the incredible swimming ability of the fish, so they endeavor to improve the performance of aquatic man-made robotic systems by using undulatory movement instead of conventional rotary propellers used in ships or underwater vehicles. This kind of propulsion is less noisy, more effective and maneuverable than propeller-based propulsion. Therefore a biomimetic robot fish might be used in many marine and military fields such as exploration of fish behavior, military reconnaissance, leakage detection in oil pipelines, seabed exploration and robotic education, etc (Hirata, 1999; Zhou *et al.*, 2008).

Many research works have been done on the propulsive theory. Marey in 1895 and Breder in 1926 were the former scientists that begun cinematography study on different methods of fish propulsion. Classical theory of Gray and his paradox (1933) created a special place in this area. Afterward, further discussions were about the maximum attainable speed of fish such as tuna fish that swim more than 20m/s and the dolphins more than 15m/s (Asadian and Abbaspour, 2013).

In 1960, a new model was built by Lighthill based on elongated body theory to analyze the carangiform propulsive mechanism (Lighthill, 1960), and the large amplitude elongated body theory (Lighthill, 1971) was propounded to analyze the irregularly amplitude of tail (Lighthill, 1969; Lighthill, 1970). Some experiments on hydrodynamics of fish movement with DPIV technique are made by Lauder *et al.* (2002), which allows empirical analysis of force magnitude and direction. They examined fin function in four ray finned fishclades; sturgeon, trout, sunfish and mackerel (Lauder *et al.*, 2002).

The first fish-like robot with eight-link, RoboTuna, has been successfully developed by MIT. Subsequent RoboPike were used to study drag reduction in fishlike locomotion. Later, an improved version of RoboTuna, Vorticity Control Unmanned Undersea Vehicle (VCUUV), was constructed by Draper Laboratory of MIT. The VCUUV was equipped with many different sensors, and could realize up-down motion and avoid obstacles, which allow it to be able to navigate autonomously in a 3-D workspace (Anderson *et al.*, 1997).

Various types of aqua robotic activities took place to develop the efficiency of underwater machines. For example, since 1999, Japan Maritime Research Institute built prototype fish robots (PPF-01 to PPF-09) to show the mechanical design and control system of robots (Hirata, 2000).

\*Corresponding Author Email: [m.asadian@gmail.com](mailto:m.asadian@gmail.com)

Designing and manufacturing of three robot fish covered with shiny flakes has been done at Essex University in England. These robots are 50 cm long, 15 cm height and 12 cm wide. Shape Memory Alloy (SMA) was used in eel type robot at Marine Science Center of Northeastern University and depth control performed by lateral body wave (Radmard, 2009). However, most former researchers focused on robotics science and less consideration was made on optimization of motion equation based on real fish swimming. The technical novelty of this paper lies in analysis of the carangiform propulsive wave curve and the design of tail mechanical structure.

## MATERIALS AND METHODS

### Basic fluid dynamic principles

There are three non-dimensional numbers that have important influence on kinematics and hydrodynamics of fish swimming: Reynolds number, Strouhal number and shape number.

Reynolds number (Re) shows the ratio of inertial to viscous forces in a flow:

$$Re = \frac{\rho UL}{\mu} \quad (1)$$

In fish swimming,  $\rho$  is the density of the water,  $L$  a fish length, and  $U$  a progressive velocity of fish. In practice, Re is only useful as an order of magnitude and high Re number, more than 300 or so, means that viscosity is not very important but has several important consequences such as wake, vorticity, added mass and turbulent flow which may change many of the standard rules of thumb of fluid dynamics, like drag and lift coefficients.

Fish generates a reverse Karman vortex street in its backward wake of the flow by oscillating of body and

caudal fin. This phenomenon is independent of the Reynolds number but depends strongly on the Strouhal number:

$$St = \frac{fA}{U} \quad (2)$$

Where  $f$  is the tail beat frequency,  $A$  is the width of the wake or the mean lateral excursion of the caudal fin at the trailing edge and  $U$  is forward swimming speed. In fish free swimming, St Number almost lies between 0.25 and 0.35 to have more effective propulsion force. In most experiments;  $A$  is assumed to be constant. So, fish changes its frequency for keeping the St Number in the above range indifferent velocities.

In this paper, Shape number define as ( $L_f/L$ ), the ratio of fore part of the fish which has the minimum amplitude in undulatory movement to the total length of the fish (Fig. 1).

### Experimental setup and results

#### 1. Ichthyologic basis

In this research, four *Pangasius sanitwongsei* with different size and swimming speed were selected for experiments (Table 1) and housed in 3750-liter tanks (250×150×100 cm) with circulation mechanism of fresh water at 27°C (±1°C) (Fig. 2 and 4a). *Pangasius sanitwongsei* is a freshwater fish species in the shark catfish family of order Siluriformes and native to the Mekong River basin & Chao Phraya River basin in Thailand.

They are categorized in BCF<sup>1</sup> and carangiform swimmers, and simulated robot create undulatory movement with a series of oscillatory hinge joints which are placed at the last 1/3 part of the body.

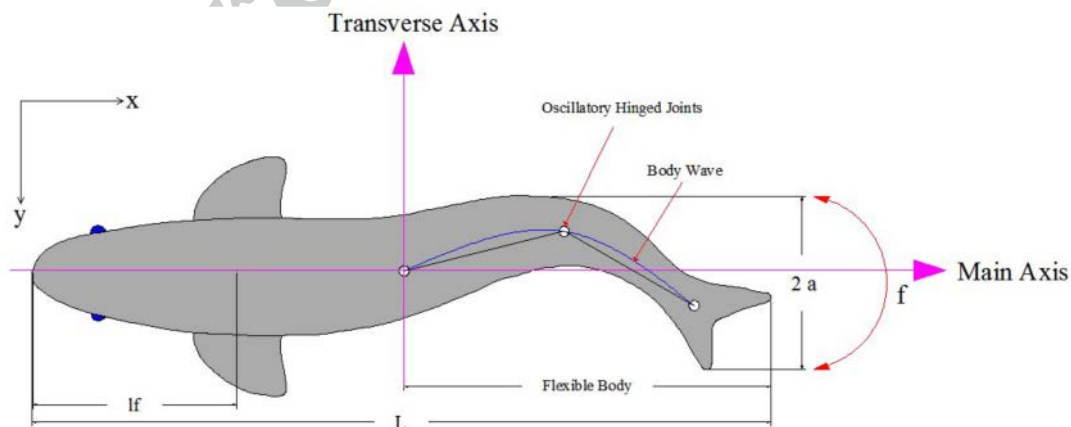


Fig. 1: Schematic of Pangasius's Deformation & Body Traveling Wave

<sup>1</sup> Body and Caudal Fin



Fig. 2: Anesthetized Pangasius with 12 cm length

Table 1: Characteristics of four Pangasius sanitwongsei with different length and velocity

	L(cm)	L <sub>r</sub> (cm)	A(cm)	f(1/s)	U(cm/s)	L <sub>r</sub> /L	St	Re
NO.1	12	3.48	3.35	1.67	11.76	0.290	0.47	14042
			2.26	1.43	9.78		0.33	11678
			2.62	1.67	10.72		0.41	12800
NO.2	9	2.52	1.00	8.33	48.46	0.280	0.17	43397
			2.95	6.25	51.00		0.36	45672
			1.20	8.33	48.44		0.21	43379
NO.3	7.5	2.03	0.96	5.00	19.52	0.270	0.25	14366
			1.10	8.33	25.92		0.35	19343
			1.00	5.00	24.17		0.21	18037
NO.4	5.8	1.51	1.35	3.12	11.38	0.260	0.37	6568
			1.82	4.17	16.50		0.46	9569
			1.17	3.55	12.50		0.33	7260

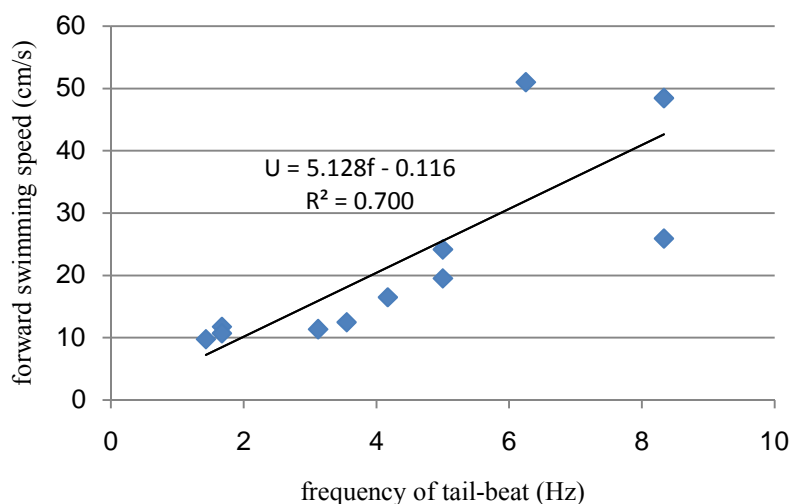


Fig. 3: Relationship between speed and frequency of tail-beat

Fish were fed with commercial pellets daily and acclimated to laboratory conditions for one week before experiments. They were lightly anesthetized by standard medicine to allow morphological measurement shown in Table 1. In Table 1, we show the result of some experiments on various Pangasius's

as a sample; the precise results and discussion on movement were shown on further section.

Fig. 3 shows the relationship between progressive velocity (U) and frequency of tail-beat (f) of Pangasius's. It is clear from this graph that the relationship between speed and frequency down to

about 5 beats per second could be represented by a straight line same as other references (Bainbridge, 1957) and also shows that the larger fish travels faster at any given frequency. The frequency of the propulsive cycle ( $f$ ) increased linearly with speed (Fig. 3) with a significant correlation according to the Eq. 3:

$$U = 5.128 f - 0.116 \quad (3)$$

### 2. Digital particle image velocimetry setup

Hydrodynamics and kinematics characteristics of four Pangasius were derived by DPIV<sup>1</sup> method. In this method, as shown in Fig. 4b, there are high speed camera (Cube 3 up to 128,000 fps) above the test tank (90×45×30 cm) with optical instruments such as 4,000mW Nd-Yag laser ( $\lambda=532\text{nm}$ ), plano-convex cylindrical lens, plano-concave lens, laser-induced fluorescent particles.

Laser produces a horizontal green light sheet at the 45° front-surface mirror positioned below the test tank and the camera captures the fish in light sheet at 100 fps from above, then photos analyze in image processing code precisely and several characteristics such as posture, trajectory and swimming mode were derived.

In carangiform fish, we assumed that body midline take the form of a sinusoidal traveling wave from the head to the tail's fin given by (4 and 5) (Lighthill, 1960):

$$y_{body}(x, t)A(x) \sin(kx\omega t) \quad (4)$$

$$A(x)[C_0 + C_1xC_2x^2] \quad (5)$$

$Y_{body}$ : Transverse displacement of body and caudal

fin cm.

$A(x)$ : Second order function described as wave amplitude cm.

$x$ : Displacement along main axis cm.

$k = 2\pi/\lambda$  Body wave number Radian.cm<sup>-1</sup>.

$\lambda$ : Wavelength of body wave cm.

$C_0$ : constant coefficient.

$C_1$ : Linear wave amplitude envelope.

$C_2$ : Quadratic wave amplitude envelope.

$\omega = 2\pi f = 2\pi/T$  Body wave frequency Radian.s<sup>-1</sup>.

## RESULTS AND DISCUSSION

As a sample, Fig. 5 displays nine selected images of 9 cm Pangasius which is taken consecutively at  $f = 50$  Hz and  $\Delta t = 18$  msec. These images reveal undulatory movement of fish in one wavelength (mean  $\lambda = 6.18$  cm). Times between tracings are in milliseconds so each image sequence was about 2 msec. The steady swimming speed of this Pangasius was recorded at mean  $5.38 \text{ L.s}^{-1}$  and thrust is produced by means of a rather stiff caudal fin and oscillating body wave.

We use DPIV method for other Pangasius's with different length, beat frequency and velocity too. According to this method, both transverse displacement of body and longitudinal movement along main axis are derived for each fish (Fig. 6), so the mean value of  $C_1$  and  $C_2$  coefficients of movement are obtained for each fish in its cycle and second order function described as wave amplitude at time-averaged movement is denoted as Table 2 for various Pangasius's. In Table 2, we show the mean value of amplitude, beat frequency and St Number of four various Pangasius's in approximate condition of experiments.

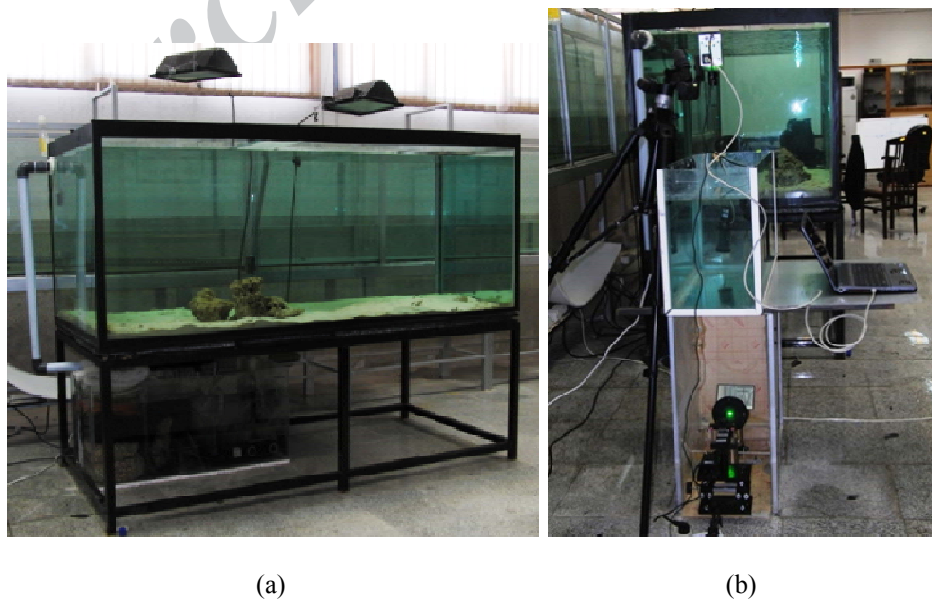


Fig. 4: Experimental apparatus in Science and Research Branch, Islamic Azad University (IAU): (a) Pangasius's maintenance aquarium in laboratory (b) Digital Particle Image Velocimetry (DPIV) Setup.

Table 2:  $C_1$  and  $C_2$  coefficients of wave amplitude at time-averaged movement of four Pangasius's

	L(cm)	$C_0$	$C_1$	$C_2$	A(cm)	f(1/s)	U (L/s)	St
NO.1	12	-25.73	11.51	-1.12	1.84	8.64	4.71	0.281
NO.2	9	-1.98	1.49	-0.13	1.72	7.74	5.45	0.252
NO.3	7.5	-17.96	9.29	-1.00	1.02	6.11	3.09	0.269
NO.4	5.8	-55.38	19.13	-1.55	1.45	3.61	2.55	0.353

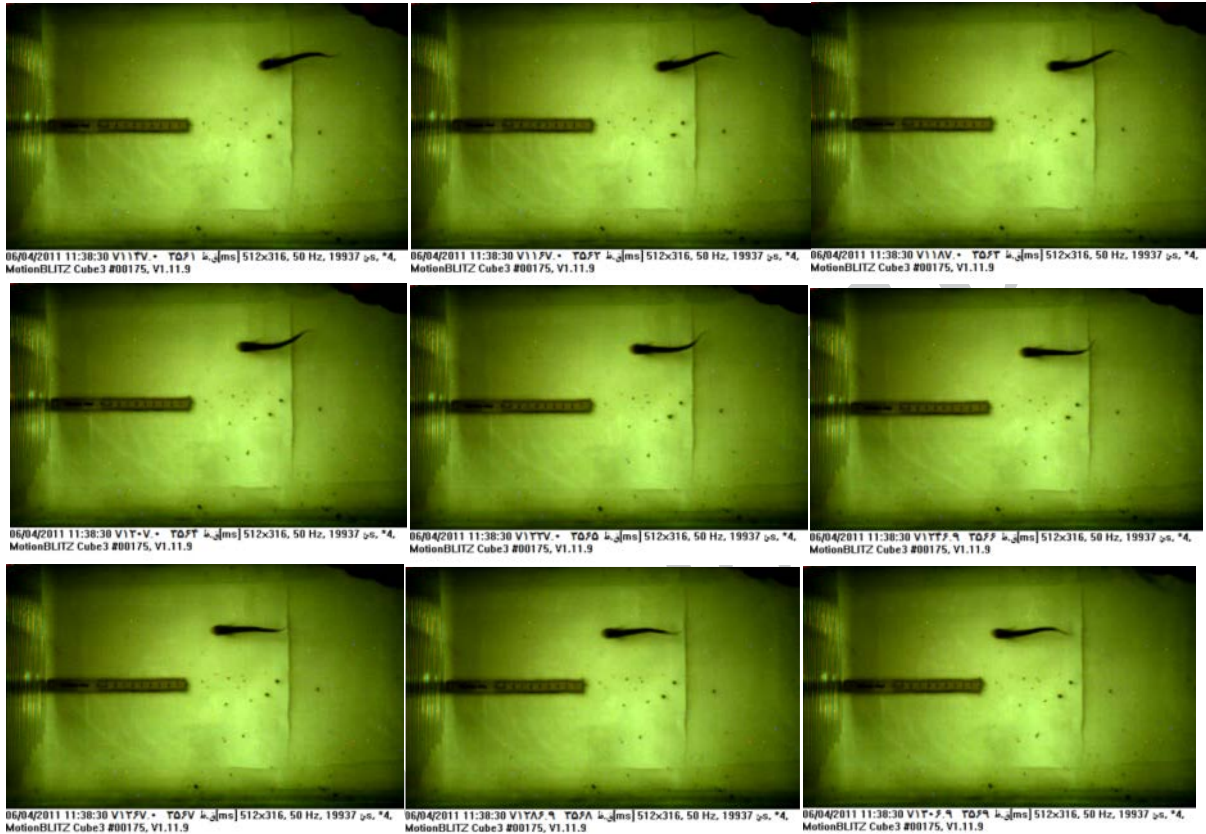


Fig. 5: Nine selected images of Pangasius by  $L=9\text{cm}$  at interval  $\Delta t = 18$  msec.

**CONCLUSION**

According to several experiments done on various Pangasius's, we realized that there are three important parameters influenced on velocity control algorithms and body wave traveling of robot fish: frequency of body wave, amplitude of the posterior body wave and length of the undulating part. The non-dimensional St Number of fish shows the combination effect of amplitude and frequency in fish swimming and in this research; we show that tail wave amplitude is the most parameter in steady swimming of fish.

It is observed that real fish in nature use a combination of frequency and amplitude for speed control. Swimming speed increases with the oscillating  $f$ , and  $f$  will approximate a constant when the desired speed is achieved. This algorithm was adopted by MIT's RoboTuna and DRAPER's VCUUV.

In practice, a second order function obtained in present experiments is the basis of speed control method and adjusts the transverse movement of robot

at a constant oscillating frequency. The amplitude of body wave is controlled by  $C_1$ , and the second-order derivative is controlled by  $C_2$ , Fig. 6 shows some envelope of the body wave with different  $C_1$  and  $C_2$ .

According to these experimental results, the maximum wave amplitude for various Pangasius's is about 1.82 cm in tail and it does not exceed fifteen percent of its body length. So, Fig. 7 shows that oscillating amplitude increases dramatically from 1/3 of body and is very small near the head.

According to the observation on real Pangasius's, not all oscillation parts of body take part in the thrust production at all time. In most of time, only 1/3 posterior portion or especially only the caudal fin oscillates to produce thrust. In a general way, with the decrease of the length ratio of the Pangasius's oscillatory part to that of the fish-body, efficiency and velocity of fish swimming remarkably increase, but maneuverability reduces to a certain extent. Otherwise, the number of simplified joints in

oscillatory part is too important in robot design, so increasing the joints causes the better mechanism's

maneuverability and redundancy, but the worse swimming efficiency.

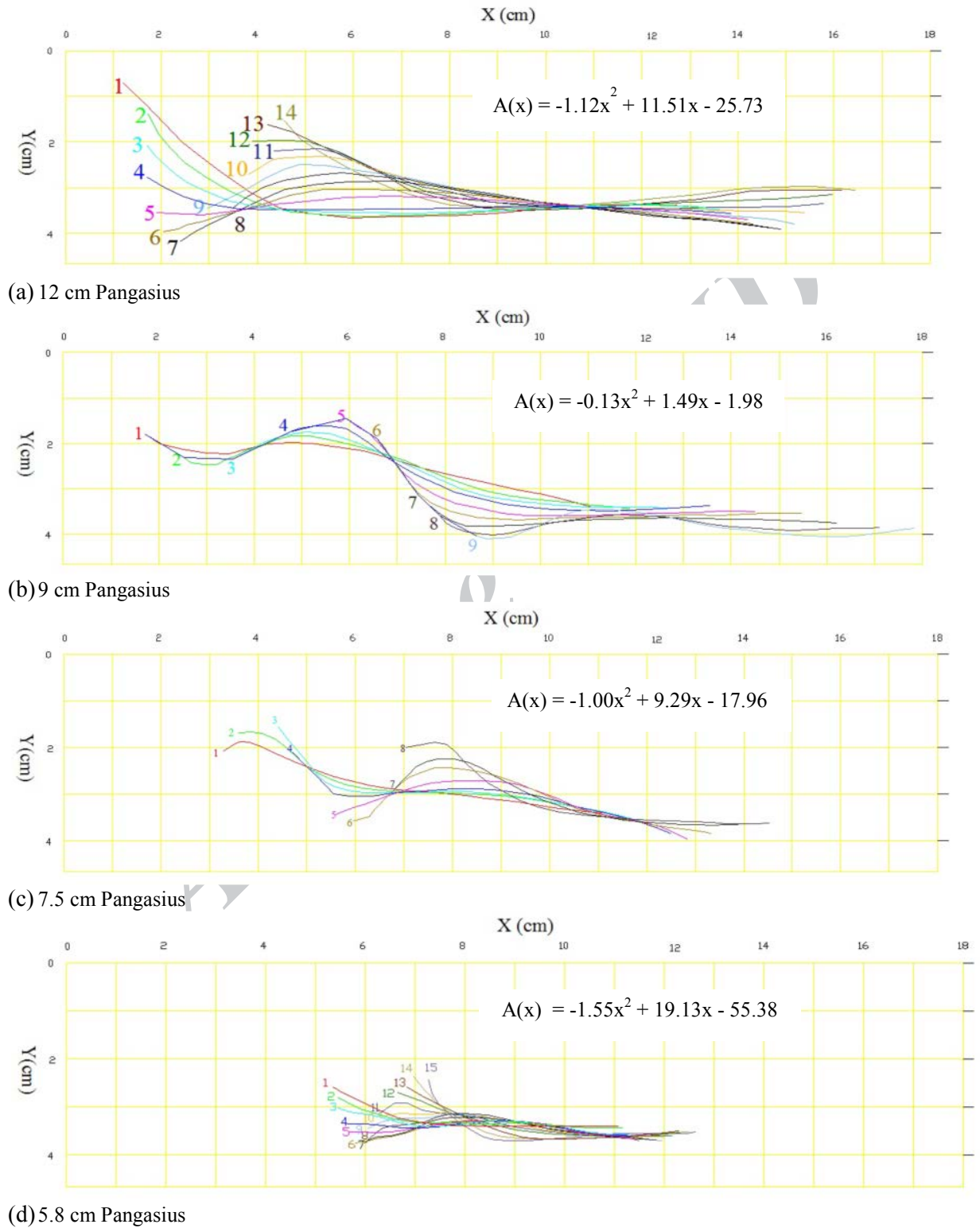


Fig. 6: Midline sinusoidal traveling body waves of four Pangasius

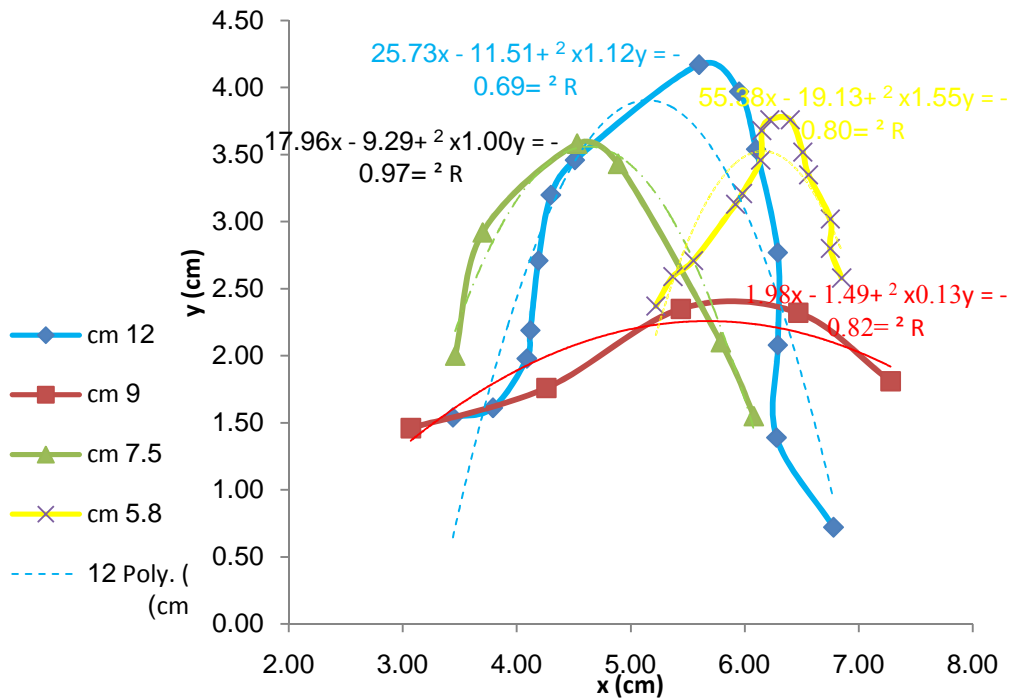


Fig. 7: Tail Traveling Waves & Second Order Polynomial of Wave Amplitude of four Pangasius

According to Fig. 7; tail traveling wave of Pangasius's have the sinusoidal form and they were acceptable by all assumptions in other references. On the other hand, we obtain new procedure for simulation of body traveling wave of robot fish and the best position of body hinges. We simulate the amplitude of the traveling wave into two parts. The first part, from the nose to the 1st hinge near the pectoral fin, which is shown in Fig. 1 with  $I_f$  that has similarity with quadratic wave amplitude envelope and the second part from  $I_f$  to end of the tail shown with linear wave amplitude envelope. We propose 3 joints for second part of robot to create a smooth and controllable motion because in each period the sinusoidal motion of robot can be formed properly.

#### ACKNOWLEDGMENTS

The authors would like to express appreciation to Dr. A.H. Javid, President of Marine Science & Technology faculty of Science and Research Branch, Islamic Azad University (IAU), for his technical assistance in laboratory.

#### REFERENCES

Hirata, K., (1999). Design and Manufacturing of a Small Fish Robot, proc. of Japan Society for Design Engineering, 99, 29-32.  
 Zhou,C.; Tan, M.; Gu, N. Z.; Cao, S.; Wang, L., (2008). The Design and Implementation of a

Biomimetic Robot Fish, International Journal of Advanced Robotic Systems, 5 (2).  
 Asadian Ghahferokhi, M.; Abbaspour, M., (2013). Experimental Hydrodynamics Analysis of Trout Locomotion for Simulation in Robot-Fish, Journal of Basic and Applied Scientific Research, 3 (4), 221-226.  
 Lighthill, M. J., (1960). Note on the swimming of slender fish, Journal of Fluid Mechanics, 9, 305-317.  
 Lighthill, M. J., (1969). Hydromechanics of aquatic animal propulsion, Annul Rev. Fluid Mech. 1, 413-447.  
 Lighthill, M. J., (1970). Aquatic animal propulsion of high hydro mechanical efficiency, J. Fluid Mech. 44, 265-301.  
 Lauder, G. V.; Nauen, E. G.; Drucker, E., (2002). Experimental hydrodynamics and evolution: function of median fins in ray- finned fishes. I. & C. Biology, 42 (5), 1009- 1017.  
 Anderson, J. M.; Triantafyllou, M. S.; Kerrebrock, P. A., (1997). Concept design of a flexible-hull unmanned undersea vehicle, Proceedings of the 7th International Offshore and Polar Engineering Conference, 82-88.  
 Hirata, T., (2000). Welcome to fish robot home page. Available at: <http://www.nmri.go.jp/eng/khirata/fish/>  
 Radmard, M. (2009). Design, modelling and control of fish robot using smart muscles. M.Sc. Thesis,

- Sharif University of Technology, Iran.
- Bainbridge, J., (1957). The speed of swimming of fish as related to size and to the frequency and amplitude of the tail beat. zoological laboratory, Cambridge, 109-133.
- Lighthill, M. J., (1960). Note on the swimming of slender fish. *Journal of Fluid Mechanics*, 9, 305–317.

**How to cite this article: (Harvard style)**

*Abbaspour, M.; Asadian Ghahferokhi, M., (2013). Simulation and optimization of live fish locomotion in a biomimetic robot fish. Int. J. Mar. Sci. Eng., 3 (1), 17-24.*

Archive of SID